Human Paleontology and Prehistory (Palaeoanthropology)

New anthropological data from Cussac Cave (Gravettian, Dordogne, France): *In situ* and virtual analyses of Locus 3

Nouvelles données anthropologiques pour la grotte de Cussac (Gravettien, Dordogne, France) : analyses in situ *et virtuelle des restes squelettiques du Locus 3*

Coralie Peignaux [a], Sacha Kacki [a,b], Pierre Guyomarc'h [c], Eline M.J. Schotsmans [a,d], Sébastien Villotte [a,*]

[a] *PACEA, UMR 5199, CNRS, Université de Bordeaux, bâtiment B8, allée Geoffroy-Saint-Hilaire, CS 50023, 33615 Pessac cedex, France*
[b] *Department of Archaeology, Durham University, South Road, Durham DH1 3LE, United Kingdom*
[c] *ADES, UMR 7268, Anthropologie bioculturelle, Droit, Éthique et Santé, Aix Marseille Université, CNRS, EFS, Faculté de médecine secteur nord, 51, boulevard Pierre-Dramard, 13344 Marseille cedex 15, France*
[d] *Centre for Archaeological Science, University of Wollongong, Northfields Avenue, Wollongong, NSW 2522, Australia*

ARTICLE INFO

ABSTRACT

Cussac Cave presents a unique combination of parietal art and several hundred parts of scattered human remains, dated to the Middle Gravettian (29–28,000 cal BP). The cave is protected as a National Heritage site. As a result, only noninvasive bioanthropological analyses are allowed, consisting of *in situ* observations and the study of 3D models obtained by photogrammetry. Here we present the first results of these analyses of the human remains from Locus 3. Only 65 of the 106 human skeletal fragments and bones could be firmly identified. Virtual analyses were carried out on 3D models of 16 skeletal elements so that osteometric data could be provided. Despite the limitations inherent in studying commingled remains and those specific to Cussac Cave, the search for virtual pair-matching, articular congruence, and osteometric sorting allowed the allocation of twelve bones to three individuals, one late adolescent and two adults.

© 2019 Académie des sciences. Published by Elsevier Masson SAS. This is an open access article under the CC BY-NC-ND license (http://creativecommons.org/licenses/by-nc-nd/4.0/).

RÉSUMÉ

La grotte de Cussac abrite une combinaison unique d'art pariétal et de centaines d'ossements humains disséminés à même le sol, datés du Gravettien moyen (29–28 000 cal BP). La grotte est classée au titre des Monuments historiques et seules des analyses non invasives (observations *in situ* et études de modèles 3D obtenus par photogrammétrie) sont autorisées. Nous présentons ici les premiers résultats de ces analyses pour le locus 3. Seuls 65 des 106 fragments squelettiques et os peuvent être formellement identifiés. Les analyses virtuelles ont pu être menées sur 16 modèles 3D permettant la production de données ostéométriques. Malgré les limites inhérentes à l'étude des vestiges mélangés et celles spécifiques à la grotte

---

* Corresponding author. Bâtiment B8, allée Geoffroy-Saint-Hilaire, CS 50023, 33615 Pessac cedex, France.
E-mail address: sebastien.villotte@u-bordeaux.fr (S. Villotte).

de Cussac, la recherche virtuelle d'appariements, de congruence articulaire et d'associations par données métriques a permis d'attribuer douze de ces os à trois individus (un grand adolescent et deux adultes), pour lesquels les principales caractéristiques biologiques sont établies.

1. Introduction

Cussac Cave is located in the commune of Le Buisson-de-Cadouin (Dordogne, France). The entrance of the cave has been known since the 1950s (Peyrony, 1950), but the karstic network, which is a 1.7-km-long gallery subdivided into two branches, called the upstream and downstream branches, was explored for the first time in September 2000 (Delluc, 2000; Jaubert et al., 2017). A series of engravings (several hundred finger-tracings and figurative and non-figurative engravings), preserved prehistoric floors, and exposed human remains were identified (Aujoulat et al., 2001; Jaubert et al., 2017). All traces of human activities (engravings, footprints, human bones) are dated back to the Middle Gravettian (29–28,000 cal BP) (Jaubert et al., 2017).

Human bones are concentrated in three areas in the downstream branch, called Loci (Aujoulat et al., 2001, 2002; Guyomarc'h et al., 2017; Henry-Gambier et al., 2013; Jaubert et al., 2017; Villotte et al., 2015). The human bones rest on the substrate, some of them being partially or totally covered with clay but still identifiable (Guyomarc'h et al., 2017; Henry-Gambier et al., 2013; Villotte et al., 2015). Because of the clay, other human remains might not have been discovered yet.

Loci 1 and 3 contain mixed remains of several individuals, while Locus 2 holds the skeleton of a single individual (Guyomarc'h et al., 2017; Henry-Gambier et al., 2013; Villotte et al., 2015).

The exceptional nature of the discovery motivated the decision to classify the cave as a National Heritage site in 2002 (Fourment et al., 2012). It is therefore subject to strict conservation measures, including the following ones:

- the cave is closed to visits, except for scientific investigations; access to the cave is limited for health hazard to the periods when the partial pressure of carbon dioxide in the cave is below 2% (ca. mid-November to mid-May);
- platforms and marked paths have to be used by the research team in order to preserve the floors that have remained untouched since the last animal or human presence;
- no conventional (i.e. invasive) archaeological investigation is currently allowed;
- high-definition photogrammetric surveys of the cave were carried out to allow noninvasive studies.

These specific study conditions in Cussac limit the analyses of the bioanthropological material drastically (Guyomarc'h et al., 2017; Villotte et al., 2015). Human remains are located several meters away from the authorized paths. Hence, the analysis is restricted to remote observations and to the study of photographs, both limited by several factors (limited light, extensive viewing distance for some clusters of remains, and bones partially or totally covered with clay).

The current study provides additional observations from a virtual study of 3D photogrammetric models of skeletal remains towards better understanding of the Cussac human remains and by extension, Gravettian biology and culture. This article focuses on results for Locus 3. The aims were to verify the minimum number of individuals (MNI) for this locus, to propose re-associations for the subjects, and to provide the scientific community with unpublished osteometric data for these bones.

2. Material and methods

Of the three loci hosting human remains, Locus 3 is the furthest away in the karstic network, 210 m from the entrance. While Loci 1 and 2 are well-defined areas easily observable from the authorized paths, Locus 3 consists of a vast area of ca. 15 square meters with a complex topography, located in a meander. Most of the area is occupied by a massif of clay associated with a large stalagmitic mass. The front part, where the current path runs, was drained a long time before the Gravettian occupation. Locus 3 can be divided into three main areas:

- an upper part where bones rest at the bottom of small depressions (which is difficult to clearly observe from the path);
- slope where more or less complete bones are scattered;
- the bottom of the slope where a few human remains are visible.

The bones look mainly well-preserved, especially compared to those of Locus 1 (Henry-Gambier et al., 2013).

The current anthropological study combines data from *in situ* observations, examination of photographs (sometimes taken with a selfie stick) and the analysis of 3D photogrammetric models of the bones. Moreover, one bone (the humerus L3-088, that rested isolated at the base of Locus 3) was collected in 2014, analyzed in laboratory, scanned, and reintroduced in the cave in 2017.

Visual observations have been made on a yearly basis by the anthropological team, usually every January since the creation of the "Projet collectif de recherche" (Joint Research Program) in 2010. The different loci were photographed from as many different angles as possible in order to determine more precisely the nature of the fragments, but also to compute high-definition 3D models. Points clouds were meshed and scaled using local physical

scales and topographic points (with *x*, *y*, *z* coordinates, acquired by a Leica© total station). After calibration (see Guyomarc'h et al., 2017 for the applied methods), the models were exploited in polygon file format (.ply), which allows for the storage of both shape and texture. The different human bones were extracted from the global model of the locus in order to allow for their detailed study in a virtual environment. The validity of the virtual measurements obtained was tested for the individual of locus 2: comparison between data obtained *in situ* on the coxal bones of this subject and those obtained from the 3D models indicated a negligible measurement uncertainty, i.e. 2.4% on average (Guyomarc'h et al., 2017).

Conventional anthropological measurements (Bräuer, 1988) have been adapted to be measured on 3D models with TIVMI software (Treatment and Increased Vision for Medical Imaging, version 2.5). Each measurement required a specific protocol through the construction of reference planes and the projection of landmarks to mimic the use of sliding and spreading calipers. Most of the measurements performed, including the maximum lengths and widths, were semi-automated. Where relevant, some measurements were estimated, based on *in situ* photographs and by comparison with complete 3D models using MeshMixer software.

The re-association or exclusion of bones is based on multiple lines of evidence from several approaches. Following Thibeault and Villotte (2018), re-associations were considered as impossible, unlikely, possible, probable, or very probable. The first approach relies on possible re-associations based on the stage of bone maturation. The second is based on a visual comparison of the 3D models. The models were imported by pair in MeshMixer software and oriented according to reference planes (see, e.g., White and Folkens, 2005). In case of comparison of bones of the same nature, a mirror model was computed before superimposition and comparison. In case of a comparison of two elements of different nature (e.g., radius vs. ulna), the two models were re-articulated in anatomical position and compared (a mirror model was created when the bones were not from the same side). The third approach is based on asymmetry in order to exclude pairs of bones. Diaphyseal asymmetry could be very marked in Gravettian individuals, but length and articular asymmetry tend to be much lower in this group (as well as in other populations, e.g., Auerbach and Ruff, 2006; Sládek et al., 2017; Sparacello et al., 2017; Trinkaus et al., 1994). Absolute asymmetry of maximum lengths was computed as a percentage: %AA = (maximum − minimum)/(average of maximum and minimum) × 100. The last approach to re-associate bones is based on metric correlations of maximum lengths. Graphs representing the maximum length of one bone as a function of another, and the resulting linear regression with a prediction interval at a 95% threshold were generated from a sample of modern adult individuals. This sample regroups 2119 skeletons from European American, African American, and Asian ancestries from both sexes. Maximum lengths were extracted from the US Database for Forensic Anthropology, 1962–1991 (ICPSR 2581) (Jantz and Moore-Jansen, 1988) and used to compute the linear regressions and associated prediction intervals.

A sample of Gravettian individuals (see Villotte et al., 2017 for a detailed presentation) was used in order to compare Locus-3 bone measurements with those of individuals from a similar period. Both samples are exclusively composed of adult subjects. The hypotheses of associations outside the 95% prediction interval were considered unlikely; only correlations with a coefficient of determination (r^2) greater than 0.80 were further discussed.

The statures of the individuals identified from the skeletal assemblage of Locus 3 were estimated using Trotter and Gleser's (1952) equation for African-Americans, as suggested by Formicola (2003) for European mid Upper Paleolithic specimens.

3. Results

3.1. Inventory, osteometric data, and first observations

One hundred and six bones, bone fragments or teeth were identified *in situ* in Locus 3. Forty-one are fragments, with small dimensions, whose nature is uncertain. The axial skeleton is represented by ten vertebrae, eight ribs or rib fragments, two mandible fragments, and three isolated teeth. The lower limb bones (13 bones or fragments) are poorly represented with the presence of one talus, one calcaneus, a fragment of coxal bone, small femoral fragments, a fragment of tibia, and a complete (but broken) fibula. The bones of the upper limbs show a higher representation (29 elements identified) and are more complete. They include one scapula, two clavicles, six humeri or humeral fragments, three radii, two ulnae, five metacarpal, seven carpals, and three hand phalanges. Based on the presence of three right humeri (all of them having their distal half preserved), the MNI for Locus 3 is three.

The number of bones for which a virtual study was carried out is limited. For some of the bones, the measurability of the 3D models was reduced due to the presence of clay coating. Additionally, photographic coverage was insufficient to produce high-quality 3D models for some areas of Locus 3 due to the complex topography and the distance between the path and the remains. Models of well-preserved bones that were not covered by clay were also partially recorded, because their surface is in contact with the ground and could not be photographed. As a result, a subsample of 16 models was optimally used for this study (Table 1 and SI1). The measurements obtained for each bone are presented in the Supplementary material (SI2).

3.2. Identification of the first individual from skeletal maturity

Three bones clearly show signs of skeletal immaturity. This is almost certain for radius L3-020 and humerus L3-024 (Fig. 1). The distal end of the radius L3-020 is in direct contact with the diaphysis, but separated exactly where a metaphyseal line should be (Fig. 1B and SI1). Observations of humerus L3-024 are more complex due to a thick layer of clay. However, a small part of the anteromedial surface of the head, not covered with clay, reveals a groove that could be interpreted as a metaphyseal line. Moreover, photographs taken using a selfie stick clearly illustrate the

Table 1
Inventory of the 3D models investigated in this study.
Tableau 1
Inventaire des modèles 3D étudiés.

| Bone	Label	Side	*In situ* preservation	Representativeness of the 3D model
Clavicle	L3-027	Left	Sternal extremity is missing	Superior surface
Humerus	L3-024	Right	Complete	Medial surface
	L3-046	Left	Proximal third	Posterior surface
	L3-047	Right	Complete	Anterior surface
	L3-057	Right	Distal half[a]	Anterior and medial surfaces
	L3-067	Left	Distal extremity	Anterior surface
	L3-088	Left	Complete	Complete
Radius	L3-020	Right	Complete	Anterior surface
	L3-026	Left	Complete	Anterior surface
	L3-086	Right	Complete	Anterior surface
Ulna	L3-018	Right	Complete apart the head	Anterior surface
	L3-068	Right	Proximal third	Medial surface
Coxal	L3-006	Right	Fragment of ilium	Lateral surface
Fibula	L3-003	Right	Sub complete (3 fragments)	Main fragments: lateral surface; proximal fragment: medial surface
Talus	L3-013	Right	Complete	Inferior surface
Calcaneus	L3-012	Right	Complete	Lateral and inferior surfaces

[a] Indicates a poor quality of the model.
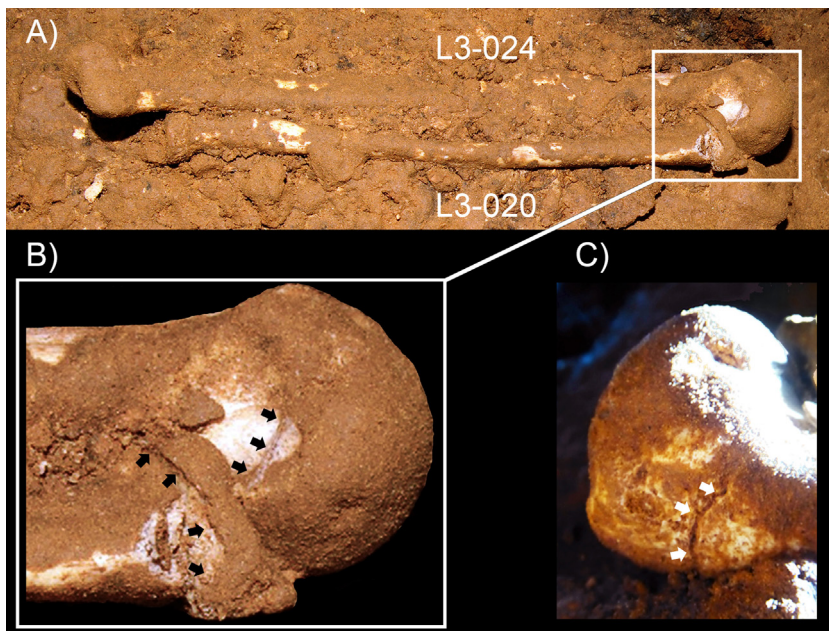
Fig. 1. Humerus L3-024 and radius L3-020 *in situ* (A), close-up of the proximal and distal extremities of these bones respectively (B), and image of the posterolateral surface of the proximal extremity of the humerus taken with a selfie stick (C). Both bones show signs of immaturity in the form of epiphyseal lines (arrows).
Fig. 1. Humérus L3-024 et radius L3-020 *in situ* (A), vue rapprochée des extrémités proximale et distale respectives de ces ossements (B), et photographie de la face postérolatérale de l'extrémité proximale de l'humérus prise avec une perche à *selfie* (C). Les deux os présentent des signes d'immaturité squelettique sous la forme de lignes épiphysaires (flèches).

metaphyseal line still visible on the posterolateral surface of the proximal extremity (Fig. 1C). Ulna L3-018 is also likely immature. The head is missing and the distal surface is eroded, but the "fracture" appears to be exactly where the metaphyseal line should be. Based on these observations, partial union for the proximal end of this humerus, and non-union of the distal extremity of the other two bones was concluded. No other sub-adult age indicator has been observed on the 3D models of Locus 3.

These three immature bones have compatible maximum dimensions (Figs. 2–4), share a similar morphology (i.e. they are relatively gracile) and compatible skeletal maturation stages (see, e.g., Schaefer, 2014). In addition, there is a good articular congruence between the radius and the ulna. The fact that these three bones belong to a single individual is therefore considered very probable. This individual was labelled Cussac L3A.
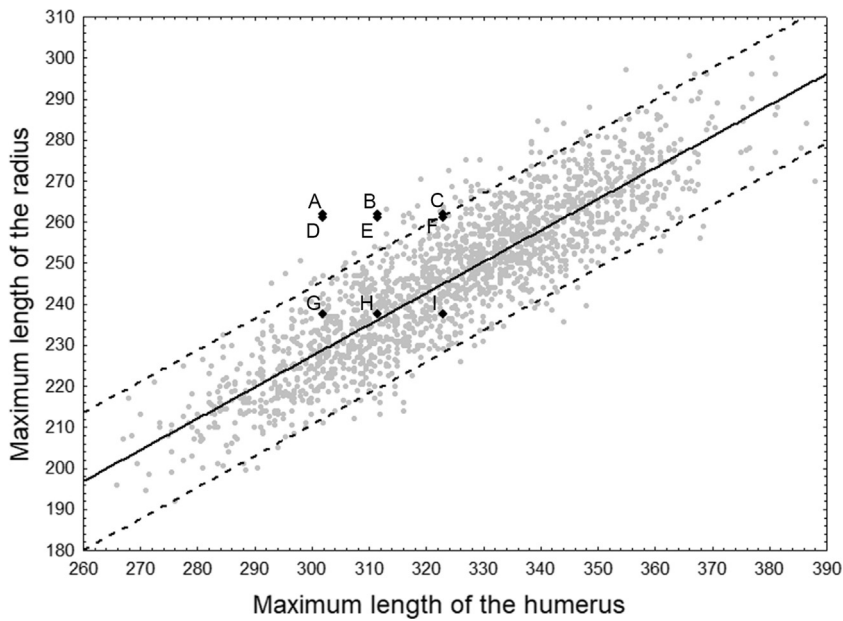
Fig. 2. Bivariate plot of the maximum lengths of the humerus and the radius, with the associated regression line and 95% prediction interval. Grey circles: modern individuals (left and right sides averaged). Black circles: tested associations (A: L3-047/L3-086; B: L3-024/L3-086; C: L3-088/L3-086; D: L3-047/L3-026; E: L3-024/L3-026; F: L3-088/L3-026; G: L3-047/L3-020; H: L3-024/L3-020; I: L3-088/L3-020).
Fig. 2. Nuage de points des longueurs maximales de l'humérus et du radius, avec la ligne de régression et l'intervalle de prédiction à 95 % associés. Cercles gris : individus modernes (moyenne des côtés droits et gauches). Cercles noirs : associations testées (A : L3-047/L3-086 ; B : L3-024/L3-086 ; C : L3-088/L3-086 ; D : L3-047/L3-026 ; E : L3-024/L3-026 ; F : L3-088/L3-026 ; G : L3-047/L3-020 ; H : L3-024/L3-020 ; I : L3-088/L3-020).
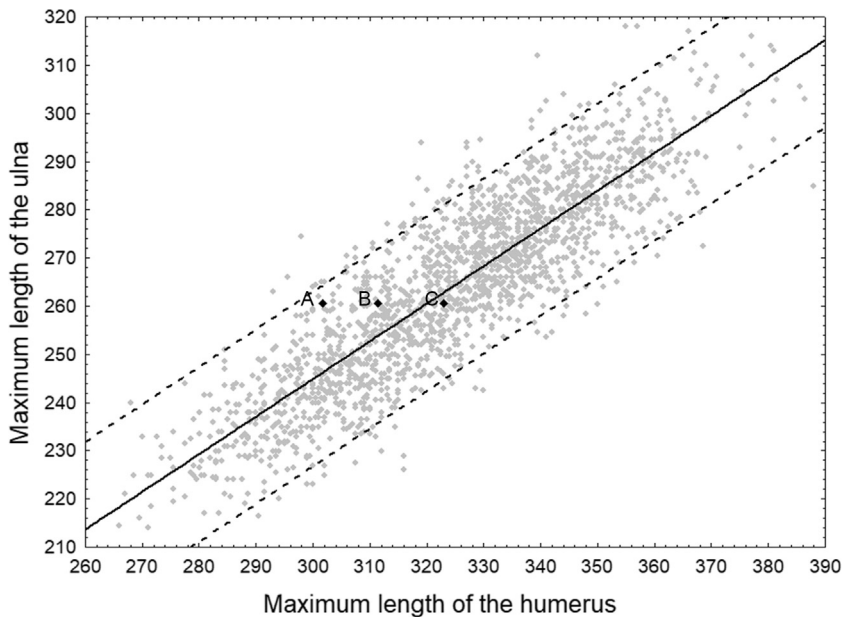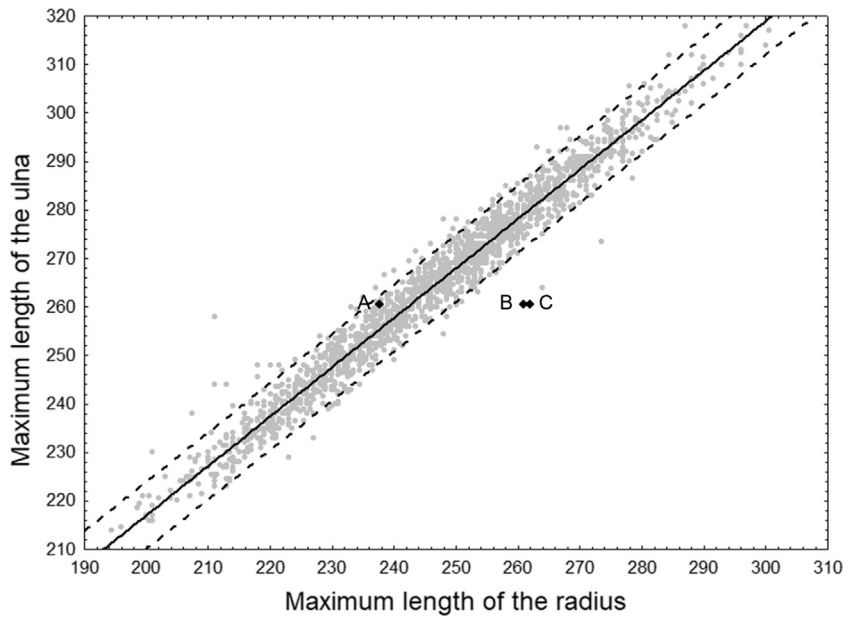

Fig. 3. Bivariate plot of the maximum lengths of the humerus and the ulna, with the associated regression line and the 95% prediction interval. Grey circles: modern individuals (left and right sides averaged). Black circles: tested associations (A: L3-047/L3-018; B: L3-024/L3-018; C: L3-088/L3-018).
Fig. 3. Nuage de points des longueurs maximales de l'humérus et de l'ulna, avec la ligne de régression et l'intervalle de prédiction à 95 % associés. Cercles gris : individus modernes (moyenne des côtés droits et gauches). Cercles noirs : associations testées (A : L3-047/L3-018 ; B : L3-024/L3-018 ; C : L3-088/L3-018).

3.3. Identification of other individuals based on humeral pair-matching

Six humeri or humeral fragments are present (Table 1), including the above-mentioned humerus L3-024 of the immature L3A, representing at least five bones (L3-046 and L3-067 may be two parts of the same bone). The humerus is the best represented and preserved bone in Locus 3 and it is, therefore, relevant for subject re-association. Nine possible pairs can be compared visually. Using the best-preserved

Fig. 4. Bivariate plot of the maximum lengths of the radius and the ulna, with the associated regression line and the 95% prediction interval. Grey circles: modern individuals (left and right sides averaged). Black circles: tested associations (A: L3-020/L3-018; B: L3-026/L3-018; C: L3-086/L3-018).
Fig. 4. Nuage de points des longueurs maximales du radius et de l'ulna, avec la ligne de régression et l'intervalle de prédiction à 95 % associés. Cercles gris : individus modernes (moyenne des côtés droits et gauches). Cercles noirs : associations testées (A : L3-020/L3-018 ; B : L3-026/L3-018 ; C : L3-086/L3-018).

bones (L3-024, L3-088, and L3-047), one impossible and one unlikely re-association, determined based on skeletal maturation stages, bone size, and bone morphology, have been recognized. L3-088, a left humerus, had been removed from the cave and studied in laboratory (Guyomarc'h et al., 2019). Its morphology is clearly different to that of L3-024, and it is a fully mature bone; their re-association is thus impossible. The re-association of L3-088 and L3-047 (a right humerus) is unlikely given their major difference in shape (Fig. 5). Moreover, they also differ significantly in size (see Table 2 in SI2), with a %AA = 6.8% for their maximum length, a percentage not seen in Gravettian individuals nor in other populations (Sládek et al., 2017). In addition to Cussac L3A, two other subjects are thus identified: Cussac L3B (humerus L3-088) and Cussac L3C (humerus L3-047).

3.4. Association of the other bones with the three defined individuals

Left clavicle L3-027 cannot be specifically assigned to any of the individuals. Indeed, the coefficient of determination (r^2) for the regression analyses that include the maximum lengths of the clavicle and humerus is low (ca. 0.55), preventing any exclusions based on robust statistical results.

The quality of the 3D model of right humerus L3-057 is poor. Based on exclusion, it cannot belong to Cussac L3A or L3C. This bone appears morphologically compatible with L3-088 (i.e. their association is considered as possible) but the allocation of this bone to Cussac L3B cannot be certain. The 3D model of left humerus L3-067, represented by its

distal end, articulates relatively well with the mirrored 3D models of the right radius L3-020 and the right ulna L3-018 (Cussac L3A). The allocation of L3-067 to Cussac L3A is considered as probable. L3-046, a proximal third of a left humerus, cannot be firmly associated with Cussac L3A or Cussac L3C.

Three radii were identified (Table 1): L3-020 (right), L3-026 (left) and L3-086 (right). The re-association of L3-020 with L3-026 is considered as impossible given the difference in maturation, as well as significant differences in size and shape. The general morphology (robustness, and orientation of the radial tuberosity) of L3-086 is compatible with L3-026. Moreover, the absolute asymmetry for the pair L3-086/L3-026 (0.4%) is comprised within the range of variations seen for Gravettian radii (from 0.4 to 3.4%, $n = 6$ pairs). The pair L3-086/L3-026 is thus considered as a probable re-association.

The maximum length of left radius L3-026 is incompatible with the ones of the right humeri L3-024 and L3-047, but it fits with the maximum length of left humerus L3-088 within the 95% prediction interval based on the modern sample (Fig. 2). Thus, following this result and the previous re-association, the pair of radii L3-026 and L3-86 probably belongs to the individual Cussac L3B. An attribution to this individual is also probable for the ulna L3-086, of which the mirrored 3D model shows a very good articular congruence with humerus L3-088.

Right coxal bone L3-006 is small (Table 2) compared to those in the Gravettian adult reference sample (i.e. the measured dimensions are inferior to the minimum available data from Gravettian females). It therefore seems likely that this bone has not fully completed his growth and could belong to Cussac L3A.

Fig. 5. Anterior view of 3D models of L3-047 (left) and L3-088 (right).
Fig. 5. Vue antérieure des modèles 3D de L3-047 (à gauche) et L3-088 (à droite).

Table 2
Comparison of the dimensions of right coxal bone L3-066 with those measured on a sample of Gravettian males and females (left and right side averaged when both present). For comparative samples: mean ± standard error, followed by the range of values in the sample (in brackets), and the number of available measurements (in parentheses).

Tableau 2
Comparaison des dimensions de l'os coxal droit L3-066 et de celles obtenues pour les échantillons gravettiens masculin et féminin (moyenne des côtés gauche et droit quand les deux sont présents). Pour les échantillons de comparaison : moyenne ± écart-type, suivie des valeurs minimum et maximum (entre crochets) et du nombre d'observations (entre parenthèses).

	Superoinferior diameter of the acetabulum	Spino-sciatic length
L3-006	45.2	63.7
Gravettian males	58.5 ± 3.0 [54.5–62.5] (9)	77.1 ± 4.6 [69.9–84.7] (10)
Gravettian females	52.6 ± 3.0 [47.3–56.2] (6)	74.5 ± 6.9 [69.0–86.0] (5)

The maximum length of fibula L3-003 appears to be compatible with the length of humerus L3-088, and radii L3-026 and L3-086; moreover, it falls outside the 95% prediction interval for the other hypotheses of re-associations (Figs. 6 and 7). Hence, re-association of this bone with individual Cussac L3B is considered possible.

Right calcaneus L3-012 and right talus L3-013 have similar dimensions, and even if their articular congruence cannot be tested, their association seems probable. Unfortunately, these two bones cannot be firmly associated with one of the three upper limb subjects.

Using a similar approach, it was not possible to re-associate with certainty the other observable bones of Locus 3 with individuals Cussac L3A, L3B or L3C, identified through their humeri. However, taking into account the elements observables *in situ* and the thorough analysis of the available photographs, there is no evidence suggesting the presence of a fourth individual.

3.5. Biological characteristics of the individuals

Cussac L3A is an immature individual represented by at least four skeletal elements: the right and left humeri L3-024 and L3-067, and right radius L3-020 and ulna and L3-018. It is possible that the right coxal bone L3-006 also belongs to this individual. Its skeletal age-at-death is estimated between ca. 15 and 19 years using current standards (e.g., Cardoso, 2008). Its stature can be estimated to ca. 1.60–1.65 m. The bones have a relatively gracile appearance.

Cussac L3B is an adult represented by at least four bones (left humerus L3-088, left and right radii L3-026 and L3-086, right ulna L3-068). The allocation of two more bones to this individual (right fibula L3-003 based on its maximum length, and right humerus L3-057 by exclusion, if the number of individuals in Locus 3 is really of three) seems possible but cannot be ascertained. Its stature is estimated to ca. 165 and 170 cm with relatively gracile bones.

Cussac L3C is represented by a single bone, right humerus L3-047. This bone seems very robust, with a short maximum length (estimated to 301.8 mm) that places
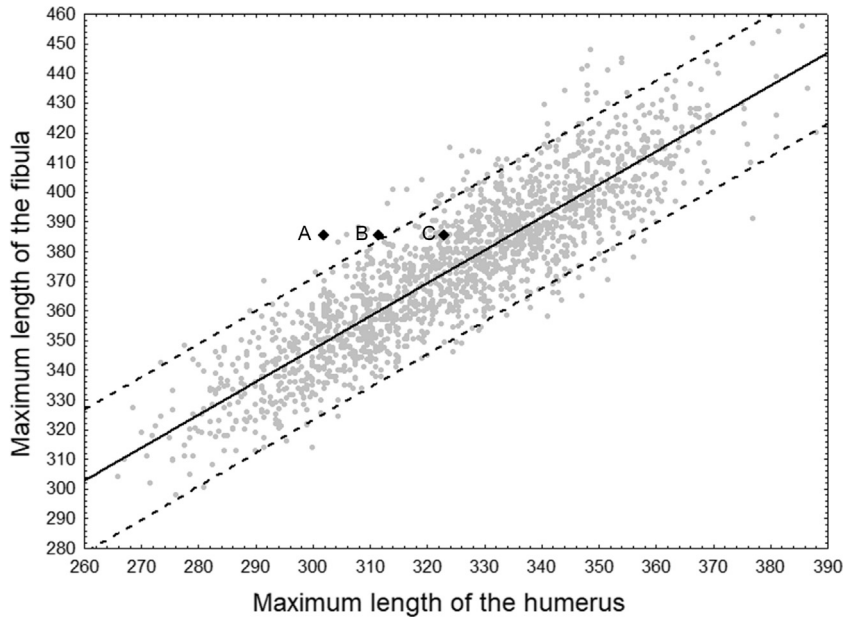
Fig. 6. Bivariate plot of the maximum lengths of the humerus and the fibula, with the associated regression line and the 95% prediction interval. Grey circles: modern individuals (left and right sides averaged). Black circles: tested associations (A: L3-047/L3-003; B: L3-024/L3-003; C: L3-088/L3-003).
Fig. 6. Nuage de points des longueurs maximales de l'humérus et de la fibula, avec la ligne de régression et l'intervalle de prédiction à 95 % associés. Cercles gris : individus modernes (moyenne des côtés droits et gauches). Cercles noirs : associations testées (A : L3-047/L3-003 ; B : L3-024/L3-003 ; C : L3-088/L3-003).
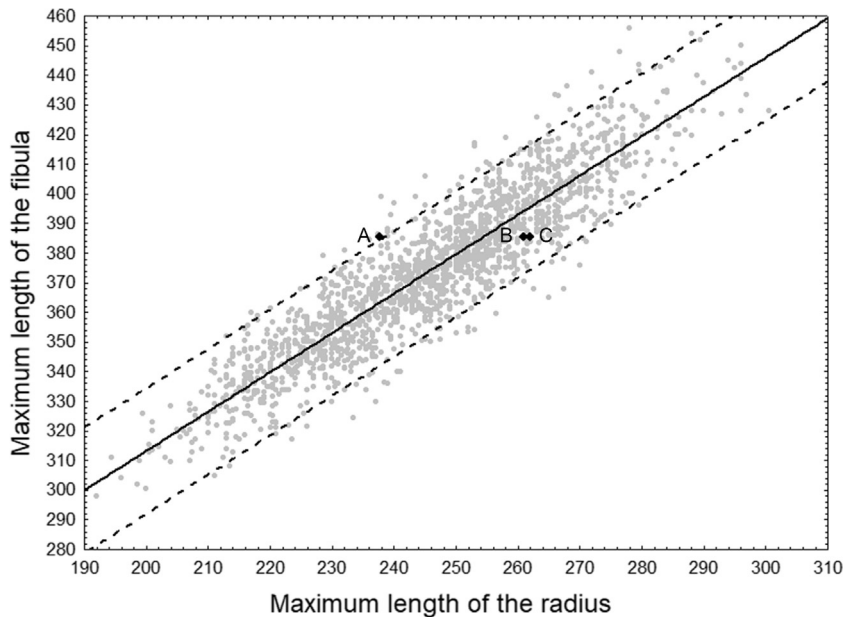
Fig. 7. Bivariate plot of the maximum lengths of the radius and the fibula, with the associated regression line and the 95% prediction interval. Grey circles: modern individuals (left and right sides averaged). Black circles: tested associations (A: L3-020/L3-003; B: L3-026/L3-003; C: L3-086/L3-003).
Fig. 7. Nuage de points des longueurs maximales du radius et de la fibula, avec la ligne de régression et l'intervalle de prédiction à 95 % associés. Cercles gris : individus modernes (moyenne des côtés droits et gauches). Cercles noirs : associations testées (A : L3-020/L3-003 ; B : L3-026/L3-003 ; C : L3-086/L3-003).

it in the lower part of the range seen for Gravettian women (316.7 ± 16.9 mm, N = 6) and at the inferior limit of the range of Gravettian men (348.5 ± 27.6, N = 12, minimum = 300).

Bones attributions are summarized in Table 3.

4. Discussions and conclusions

The analysis of human remains at Cussac Cave is limited due to strict conservation measures. We attempted, following these strict rules, to verify the MNI of Locus 3,

Table 3
Bones assigned to each individual.
Tableau 3
Ossements attribués à chacun des individus.

Degree of confidence	Cussac L3A	Cussac L3B	Cussac L3C
High	Right humerus L3-024, left humerus L3-067, right radius L3-020, right ulna L3-018	Left humerus L3-088, right radius L3-086, left radius L3-026, right ulna L3-068	Right humerus L3-047
Medium	Right coxal bone L3-006	Right fibula L3-003, right humerus L3-057	

and to allocate bones to the individuals, based on *in situ* observations, photographs, and 3D models. To our knowledge, this study is the first attempt to identify individuals from a commingled skeletal assemblage without any physical intervention. Normally the analysis of commingled remains is based on excavation data, followed by several types of analysis in the laboratory, such as bone sorting, counting, visual pair-matching, re-articulation, processes of elimination, osteometric comparison, taphonomy, or even DNA analyses (e.g., Adams and Byrd, 2006). Even this process is considered as long and difficult with limited results. Added to the many difficulties of the "conventional" study of commingled remains, the conservation measures applied at Cussac limit the study even more drastically: a vast majority (85%) of the 106 bones or fragments of bones observed *in situ* in Locus 3 cannot be virtually studied, and a significant part of them (39%) cannot even be firmly identified. Moreover, with the exception of humerus L3-088, which has been removed from the cave, the usable 3D photogrammetric models are not fully representative of the preservation of the skeletal elements. Some parts of the bones cannot be virtually reconstructed as they are covered with thick layers of clay or are simply impossible to photograph (e.g., surfaces of the bones in contact with the ground), which makes it impossible to perform measurements and limits the number of re-associations.

The current study of Cussac's Locus 3 nevertheless provides interesting initial results: nine bones were allocated with high degree of confidence to three individuals, allowing assessment of their different biological characteristics. The allocation of nine skeletal elements is based on several lines of evidence (e.g., skeletal maturation and good concordance of maximum lengths), and are thus considered as reliable. However, it should be kept in mind that the reliability of the results of this study (and future ones) depends strongly on the real number of individuals represented in Locus 3. Even if all the data acquired so far point towards only three individuals, in accordance with the assessment of the MNI that was done right after the discovery (Aujoulat et al., 2002), the presence of skeletal elements from more individuals cannot be rejected. That is the reason why we did not firmly associate more bones (i.e. the right humerus L3-057, the right coxal bone L3-006 and the right fibula L3-003) with these subjects. The likelihood of these re-associations could only be better assessed if fully representative 3D models of the bones or the bones themselves were available for study. The noninvasive approach defended by the administrative services of the French "Ministère de la Culture et de la Communication" (Fourment et al., 2012) shows its limitations: without a large-scale archeological (i.e. invasive) project,

the anthropological data for Cussac Cave will remain limited.

Funding sources

Acknowledgements

Appendix A. Supplementary material

Supplementary material (SI1 and SI2) associated with this article can be found in the online version available at https://doi.org/10.1016/j.crpv.2019.02.004.

References

Adams, B.J., Byrd, J.E., 2006. Resolution of small-scale commingling: a case report from the Vietnam War. Forensic Sci. Int. 156, 63–69.

Auerbach, B.M., Ruff, C.B., 2006. Limb bone bilateral asymmetry: variability and commonality among modern humans. J. Hum. Evol. 50, 203–218.

Aujoulat, N., Geneste, J.-M., Archambeau, C., Delluc, M., Duday, H., Gambier, D., 2001. La grotte ornée de Cussac (Dordogne). Observations liminaires. Paleo 13, 9–18.

Aujoulat, N., Geneste, J.-M., Archambeau, C., Delluc, M., Duday, H., Gambier, D., 2002. La grotte ornée de Cussac – Le Buisson-de-Cadouin (Dordogne) : premières observations. Bull. Soc. Prehist. Fr. 99, 129–137.

Bräuer, G., 1988. Osteometrie. In: Knussmann, R. (Ed.), Anthropologie: Handbuch Der Vergleichenden Biologie Des Menschen. G. Fischer, Stuttgart, pp. 160–232.

Cardoso, H.F.V., 2008. Age estimation of adolescent and young adult male and female skeletons II, epiphyseal union at the upper limb and scapular girdle in a modern Portuguese skeletal sample. Am. J. Phys. Anthropol. 137, 97–105.

Delluc, M., 2000. La grotte de Cussac. Commune du Buisson-de-Cadouin (24). Speleo-Dordogne 156, 19–24.

Formicola, V., 2003. More is not always better: Trotter and Gleser's equations and stature estimates of Upper Palaeolithic European samples. J. Hum. Evol. 45, 239–244.

Fourment, N., Barraud, D., Kazmierczak, M., Rieu, A., 2012. La grotte de Cussac (Le Buisson-de-Cadouin, Dordogne, France) : applications des principes de conservation préventive au cas d'une découverte récente. In: Clottes, J. (Ed.), L'art Pléistocène Dans Le Monde/Pleistocene Art of

the World/Arte Pleistoceno En El Mundo. In: Actes Du Congrès IFRAO (Tarascon-Sur-Ariège, septembre 2010) (Préhistoire, Art et Sociétés, LXV-LXVI 2010-11), pp. 64–65 (CD-Rom, 343–354).

Guyomarc'h, P., Samsel, M., Courtaud, P., Mora, P., Dutailly, B., Villotte, S., 2017. New data on the paleobiology of the Gravettian individual L2A from Cussac Cave (Dordogne, France) through a virtual approach. J. Archaeol. Sci. 14, 365–373.

Guyomarc'h, P., Sparacello V., Samsel M., Courtaud P., Villotte S. 2019. New biological data on a Gravettian humerus from Cussac Cave (Dordogne, France) (Submitted).

Henry-Gambier, D., Courtaud, P., Duday, H., Dutailly, B., Villotte, S., Deguil-loux, M.-F., Pémonge, M.-H., Aujoulat, N., Delluc, M., Fourment, N., Jaubert, J., 2013. Grotte de Cussac (Le Buisson-de-Cadouin, Dor-dogne) : un exemple de comportement original pour le Gravettien. In: Jaubert, J., Fourment, N., Depaepe, P. (Eds.), Transitions, Ruptures et Continuité En Préhistoire : XXVIIe Congrès Préhistorique de France, Bordeaux – Les Eyzies 31 mai–5 juin 2010. Vol. 1. Société préhistorique française, Paris, pp. 169–182.

Jantz, R., Moore-Jansen, P., 1988. A Database for Forensic Anthropology. Final Report to the National Institute of Justice, Washington, DC USA.

Jaubert, J., Genty, D., Valladas, H., Camus, H., Courtaud, P., Ferrier, C., Fer-uglio, V., Fourment, N., Konik, S., Villotte, S., Bourdier, C., Costamagno, S., Delluc, M., Goutas, N., Katnecker, É., Klaric, L., Langlais, M., Ledoux, L., Maksud, F., O'Farrell, M., Mallye, J.-B., Pierre, M., Pons-Branchu, E., Régnier, É., Théry-Parisot, I., 2017. The chronology of human and ani-mal presence in the decorated and sepulchral cave of Cussac (France). Quat. Int. 432, 5–24.

Peyrony, D., 1950. Notes sur quelques petits gisements préhistoriques. Bull. Soc. Hist. Archeol. Perigord 77, 55–57.

Schaefer, M., 2014. A practical method for detecting commingled remains using epiphyseal union. In: Commingled Human Remains. Elsevier, PL: Oxford, UK, pp. 123–144.

Sládek, V., Berner, M., Holt, B., Niskanen, M., Ruff, C.B., 2017. Past human manipulative behavior in the European Holocene as assessed through upper limb asymmetry. In: Ruff, C.B. (Ed.), Skeletal Variation and Adap-tation in Europeans: Upper Palaeolithic to the Twentieth Century. John Wiley & Sons, Inc, Hoboken, USA, pp. 163–208.

Sparacello, V.S., Villotte, S., Shackelford, L.L., Trinkaus, E., 2017. Patterns of humeral asymmetry among late Pleistocene humans. C. R. Palevol 16, 680–689.

Thibeault, A., Villotte, S., 2018. Disentangling Cro-Magnon: a multiproxy approach to re-associate lower limb skeletal remains and to deter-mine the biological profiles of the adult individuals. J. Archaeol. Sci. 21, 76–86.

Trinkaus, E., Churchill, S.E., Ruff, C.B., 1994. Postcranial robusticity in Homo. II: humeral bilateral asymmetry and bone plasticity. Am. J. Phys. Anthropol. 93, 1–34.

Trotter, M., Gleser, G.C., 1952. Estimation of stature from long limb bones of American Whites and Negroes. Am. J. Phys. Anthropol. 10, 463–514.

Villotte, S., Samsel, M., Sparacello, V., 2017. The paleobiology of two adult skeletons from Baousso da Torre (Bausu da Ture) (Lig-uria, Italy): implications for Gravettian lifestyle. C. R. Palevol 16, 462–473.

Villotte, S., Santos, F., Courtaud, P., 2015. In situ study of the Gravettian individual from Cussac Cave, Locus 2 (Dordogne, France). Am. J. Phys. Anthropol. 158, 759–768.

White, T.D., Folkens, P.A., 2005. The Human Bone Manual. Elsevier Aca-demic, Amsterdam, Boston.